J Orofac Orthop (2018) 79:427–439
https://doi.org/10.1007/s00056-018-0156-y

ORIGINAL ARTICLE

Are morphologic and topographic alterations of the mandibular fossa after fixed functional treatment detectable on tomograms? Visual classification and morphometric analysis

Gero Stefan Michael Kinzinger[1,2] · Jörg Alexander Lisson[1] · Dania Booth[1,3] · Jan Hourfar[1,4]

Received: 5 February 2018 / Accepted: 8 August 2018 / Published online: 10 September 2018

Abstract

Aim The goal was to evaluate if changes in morphology and topography of the mandibular fossa after Functional Mandibular Advancer (FMA) treatment are detectable on tomograms. Furthermore, the suitability of digital tomograms (DT) over magnetic resonance imaging (MRI) for this particular question was investigated.

Materials and methods In all, 25 patients (14 female, 11 male) with a skeletal class II malocclusion received treatment with a FMA. DTs were available prior to (T1) and after (T2) FMA treatment. A total of 50 temporomandibular joints were investigated. The mandibular fossae were evaluated metrically and visually regarding treatment-induced alterations. A $p < 0.05$ was set as the level for statistical significance for all tests. Results were compared to the results of a recent MRI study.

Results Visual inspection of all 50 joints in the DT at T1 and T2 revealed no alterations of the fossa shape in the sagittal plane; 24 patients showed identical morphology of right and left joints. The metrical analysis revealed no significant changes regarding width, depth and ratio thereof between T1 and T2. There also were no bilateral differences. Another 18 different distance measurements between porion, mandibular fossa, articular eminence and pterygoid fossa showed no significant changes. There was no detectable proof of a fossa shift.

Conclusions No changes in the sagittal plane, mandibular fossa, the articular tubercle, or a possible fossa shift were found in the DT of class II patients after FMA treatment. DT and MRI measurements and the visual inspection revealed identical findings; thus, DT appears to be a valuable research tool for sagittal analysis of mandibular fossa changes.

Keywords Functional Mandibular Advancer · Articular tubercle · Fossa shift · Temporomandibular joint · Magnetic resonance imaging

✉ Univ.-Prof. Dr. Jörg Alexander Lisson
joerg.lisson@uniklinikum-saarland.de

[1] Department of Orthodontics, Saarland University, Universitätskliniken 56, 66421 Homburg/Saar, Germany

[2] Private Orthodontic Practice, Toenisvorst, Germany

[3] Private Orthodontic Practice, Rheinberg, Germany

[4] Private Orthodontic Practice, Michelstadt, Germany

Sind morphologische und topographische Veränderungen der Fossa mandibularis durch eine festsitzende funktionskieferorthopädische Apparatur auf Tomogrammen nachweisbar? Eine retrospektive visuelle Klassifikation und morphometrische Analyse

Zusammenfassung

Zielsetzung Ziel der Studie war es zu überprüfen, ob potenzielle Effekte einer Behandlung mit einem FMA („functional mandibular advancer“) auf Morphologie und Topographie der Fossa mandibularis an digitalen Tomogrammen darstellbar sind. Ihre Eignung als diagnostisches Mittel wurde im Vergleich mit der MRT (Magnetresonanztomographie) untersucht.

Material und Methoden Fünfundzwanzig Patienten (14 weiblich, 11 männlich) mit skelettaler Klasse-II-Malokklusion wurden mit dem FMA behandelt. Tomogramme waren für den Zeitpunkt vor (T1) und nach (T2) der FMA-Behandlung verfügbar. Insgesamt wurden 100 Kiefergelenke (KGs) untersucht. Die Fossae mandibulares wurden metrisch und visuell auf mögliche therapeutisch induzierte Veränderungen hin evaluiert. Bei allen statistischen Tests wurde Signifikanz bei $p < 0{,}05$ angenommen. Die Ergebnisse der Tomogrammstudie wurden mit denen einer MRT-Studie verglichen.

Ergebnisse Die visuelle Befundung der Tomogramme zu den beiden definierten Kontrollzeitpunkten ergab bei allen 50 Kiefergelenken keine Veränderungen der Fossaform in der Sagittalebene. Zudem war bei 24 Patienten die Morphologie der Fossae bei rechtem und linkem Gelenk identisch. Die metrische Analyse zeigte keine signifikanten Veränderungen hinsichtlich Breite, Tiefe und deren Verhältnis zueinander zu den beiden definierten Kontrollzeitpunkten, auch nicht im Seitenvergleich. Weitere 18 Streckenmessungen zwischen Porion, Fossa mandibularis, Tuberculum articulare und Fossa pterygoidea ergaben bei allen 50 Gelenken weder insgesamt noch unterteilt in rechte und linke Seite noch im Seitenvergleich signifikante Veränderungen. Hinweise auf einen Fossa „shift“ gibt es nicht.

Schlussfolgerungen Bei der Behandlung mit einer starren, festsitzenden, funktionskieferorthopädischen Apparatur zur Korrektur von Distalbisslagen ergaben weder die visuelle Befundung noch verschiedene metrische Analysen an sagittalen Tomogrammen Hinweise auf morphologische Veränderungen der Fossa mandibularis und des Tuberculum articulare sowie auf einen möglichen Fossa „shift“. Da die Absolutwerte identischer Messungen an den Tomogrammen und den MRT-Aufnahmen beim selben Kollektiv vergleichbar sind und auch die visuellen Befundungen einander entsprechen, stellt in der Sagittalebene das Tomogramm eine diagnostische Alternative zur MRT dar.

Schlüsselwörter Functional Mandibular Advancer · Tuberculum articulare · Fossa shift · Temporomandibulargelenk · Magnetresonanzbildgebung

Introduction

Angle Class II, division 1 with mandibular retrognathia is the most frequent malocclusion in central Europe [8]. Orthodontic treatment usually includes removable or fixed functional appliances [7, 30]. The functional appliance treatment period is approximately 6–9 months [50]. When the functional appliance (FA) is inserted, the condyles are moved to an anterior position on the articular tubercle, which is capable of adaptation [19]. Thus, it was hypothesized that morphological changes may occur [20].

In their systematic review, Ivorra-Carbonell et al. [19] evaluated the main effects of different functional appliances on temporomandibular joints (TMJ). A total of 401 articles were identified. However, only 21 papers (1 review and 20 clinical studies) were finally included: 10 of which reported on fixed functional appliances (FFAs; [1, 17, 23, 24, 27, 28, 30, 34, 35, 50]), 10 on removable functional appliances (RFAs; [3, 4, 10, 11, 16, 20, 48, 53–55]) and 1 study compared the treatment effects of FFAs and RFAs [7]. Ivorra-Carbonell et al. [19] concluded from their review that treatment with FAs leads to a more advanced position the condyle, with remodelling of the condyle and adaptation of the morphology of the mandibular fossa. Still, the articles included in the review showed a lack of methodological homogeneity.

The TMJ is the body’s most complex joint [2]. Different two-dimensional (2D) and three-dimensional (3D) imaging modalities for TMJ diagnosis have been advocated, including plain films, cephalograms [33, 35, 41], cone beam computed tomography (CBCT), magnetic resonance imaging (MRI) and tomography [5, 9].

The most frequently investigated fixed functional appliance (FFA) treatment effects are those after treatment with a Herbst appliance [36] or Functional Mandibular Advancer (FMA; [26]). Numerous studies of FFA patients investigated therapy-induced effects upon the TMJ, particularly focusing on condylar position, morphology and discocondylar relationship [27, 28, 40, 42–47]. Although some studies investigated morphological changes of the condyles using tomograms [37], little attention has been paid towards potential changes of the mandibular fossa position and shape following FFA therapy.

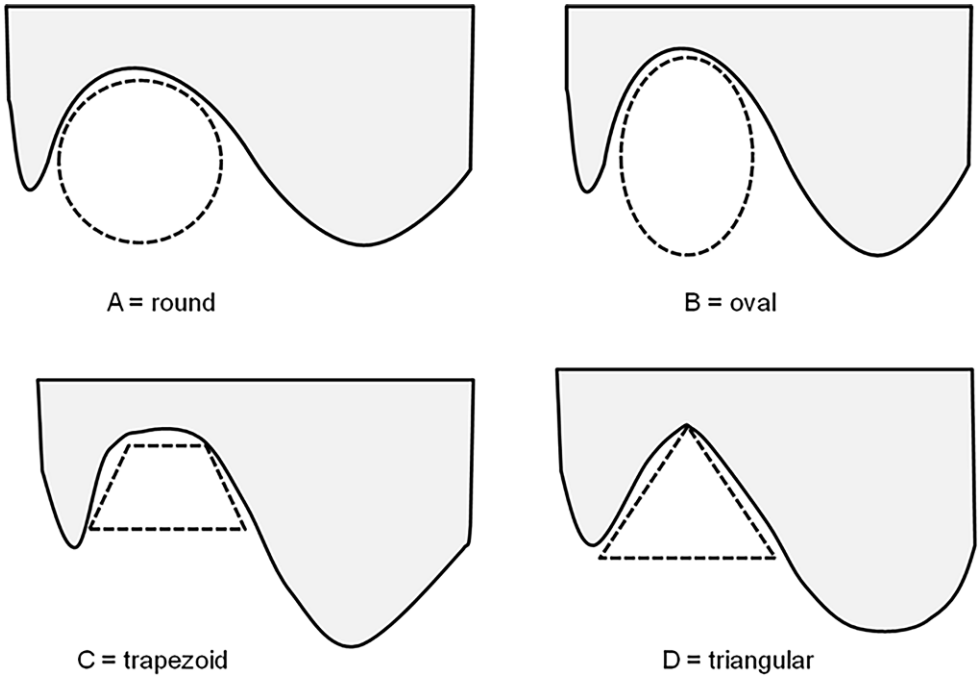

Fig. 1 Classification of mandibular fossa shape according to Katsavrias: round (A), oval (B), trapezoidal (C) or triangular (D; [21])
Abb. 1 Einteilung der Formen der Fossa mandibularis nach Katsavaris: rund (A), oval (B), trapezförmig (C) bzw. dreieckig (D; [21])

Ruf and Pancherz [43, 45] first suspected possible mandibular fossa remodelling in their investigation of Herbst appliance treatment effects. Only a few studies attempted to assess these morphologic changes of the condyles and fossae not only visually but also metrically. Kinzinger et al. [25] recently investigated possible changes of the mandibular fossae using MRI datasets. The anatomical structures were assessed visually and metrically in the sagittal plane.

Tomograms are suitable for certain aspects of TMJ diagnosis [12]. Compared to MRI scans, tomograms have the advantage that additional osseous structures anterior and posterior to the fossa mandibularis and the articular tubercle, e.g. porion or pterygopalatine fossa, can be used as reference points for different linear measurements [22]. Considering these structures as stable during the short period of functional treatment during growth, particularly the evaluation of positional changes of the mandibular fossa, the so-called fossa shift, seems feasible.

This study used tomograms to investigate the following:

- if treatment with the Functional Mandibular Advancer (FMA) led to changes in (a) shape and (b) width and depth of the mandibular fossae in the sagittal plane,
- if treatment with the FMA led to a fossa shift, i.e. changes of the topographic relation between porion, mandibular fossa, articular tubercle and pterygopalatine fossa, and
- if including porion and pterygopalatine fossa on the tomogram measurements may usefully complement MRI measurements [25].

The investigation also tested the hypothesis that visual classification of mandibular fossa shape and different linear measurements led to results comparable to those of a previously published study using MRI for the same purpose.

Materials and methods

Patients

The study included 25 patients with a skeletal Class II malocclusion (14 females, 11 males). They were the same used for a previous study (Kinzinger et al. [25]). Mean age was 16 years (range 12.0–27.6 years) at the beginning of treatment. Average functional treatment time with the Functional Mandibular Advancer (Forestadent, Pforzheim, Germany) was 7.3 months (range 6–9.5 months). All patients were treated by one experienced orthodontist and received a single-step advancement (SSA) protocol to protrude the mandible to an edge to edge position. After treatment, all patients showed a bilateral Class I molar relationship. Tomograms were available prior to (T1) and after (T2) FMA treatment.

Further inclusion criteria were the following: complete permanent dentition without third molars, no tooth loss during treatment, no history of previous orthodontic treatment, molar relationship of at least ½ cusp width distal, and pretreatment ANB angle ≥4°. Exclusion criteria were craniofacial anomalies, congenital agenesis or permanent tooth loss, or planned extraction protocol.

A total of 50 mandibular fossae measurements on parasagittal slices of MRIs of a study by Kinzinger et al. [25] served as controls for comparison.

Visual classification of mandibular fossae

The mandibular fossa shape was always assessed ipsi- and contralaterally on tomograms at T1 and T2. According to Katsavrias [21], mandibular fossa shape was recorded as either round (A), oval (B), trapezoidal (C) or triangular (D; Fig. 1).

Radiographic material and metric analysis

Always two digital tomograms (DTs) taken with the same device (Orthophos®, Sirona, Bensheim, Germany) were available for each patient. Positioning of the patients within the x-ray unit was performed according to the manufacturer's instructions using a standard bite block [14]. The first DT (T1) was taken as part of the pretreatment diagnostics. The second DT (T2) was recorded at the end of FMA treatment.

A total of 50 DTs were evaluated, for a total of 100 TMJs at T1 and T2. Metric analysis was performed by one single blinded investigator using a dedicated software (fr-win®, version 7.0; Computer Konkret, Falkenstein, Germany). This dedicated tracing software is capable of measuring to two decimal places.

The metric analysis of the mandibular fossae was performed according to Katsavrias and Voudouris [22]. Seven reference points were traced on the DTs per TMJ (Fig. 2):

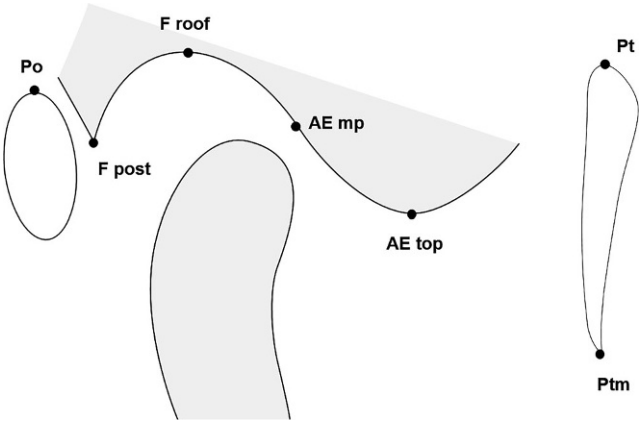

Fig. 2 Seven reference points in the sagittal plane referring to porion, mandibular fossa, articular tubercle (*AE* articular eminence) and pterygoid fossa. See text for description of points/abbreviations

Abb. 2 Sieben Referenzpunkte in der Sagittalen zur Erfassung von Porion, Fossa mandibularis, Tuberculum articulare („articular eminence", *AE*) und Fossa pterygopalatina. Messpunkte und Abkürzungen s. Text

- Porion, Po (uppermost point of auditory meatus);
- Fossa posterior, F post (the top of postmandibular process);
- Roof of the mandibular fossa, F roof (the highest point of the mandibular fossa);
- Articular tubercle midpoint, AE mp (the middle point between roof of the mandibular fossa and the height of the articular tubercle);
- Height of the articular tubercle, AE top;
- Pt (top of the pterygopalatine fissure) and
- Ptm (bottom point of the pterygopalatine fissure).

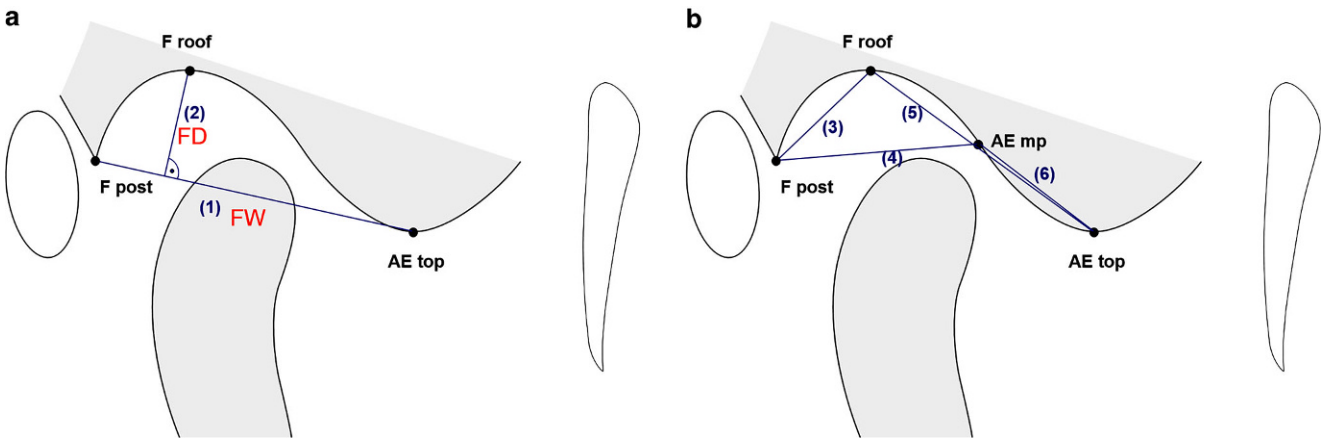

Fig. 3 **a** F post-AE top (mandibular fossa width, 1), F roof on F post-AE top (mandibular fossa depth, 2). **b** Measurements of the mandibular fossa and the articular tubercle (*AE*): F post-F roof (3), F post-AE mp (4), F roof-AE top (5), AE mp–AE top. See text for description of points/abbreviations

Abb. 3 **a** „F post-AE top" (Breite der Fossa mandibularis, 1), F roof on F post-AE top (Tiefe der Fossa mandibularis, 2). **b** Messungen an der Fossa mandibularis und am Tuberculum articulare (*AE*): F post-F roof (3), F post-AE mp (4), F roof-AE top (5), AE mp–AE top (6). Messpunkte und Abkürzungen s. Text

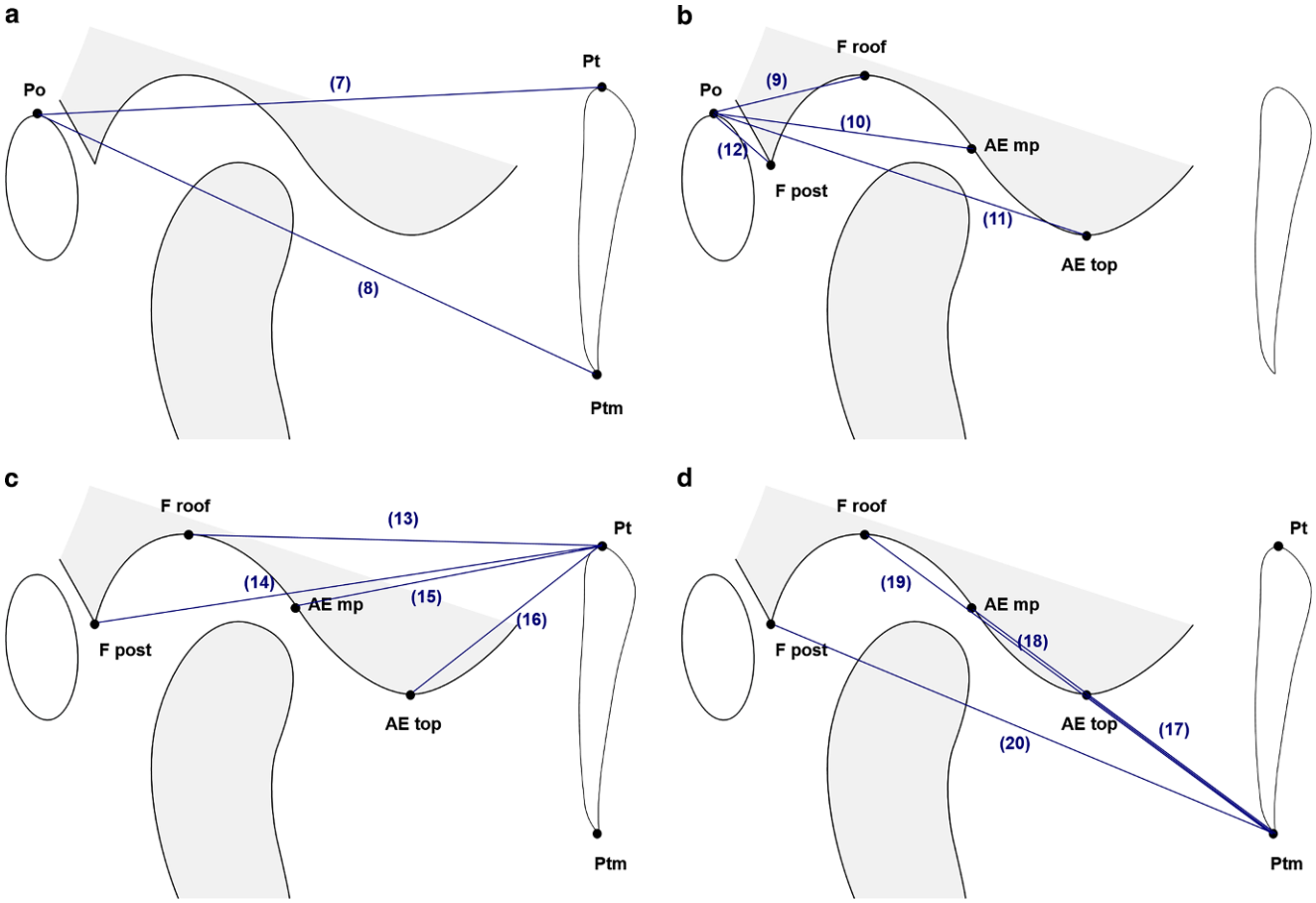

Fig. 4 **a** Measurements Po-Pt (7) between porion and pterygopalatine fossa, and Po-Ptm (8) between porion and pterygopalatine fossa. **b** Measurements between porion to mandibular fossa and to articular tubercle (*AE*): Po-F roof (9), Po-AE mp (10), Po-AE top (11), Po-F post (12). **c** Measurements between the pterygopalatine fossa (point Pt) to reference points of the mandibular fossa and to articular tubercle (*AE*): F roof-Pt (13), F post-Pt (14), AE mp-Pt (15), AE top-Pt (16). **d** Measurements between the pterygopalatine fossa (point Ptm) to reference points of the mandibular fossa and to articular tubercle (*AE*): AE top-Ptm (17), AE mp-Ptm (18), F roof-Ptm (19), F post-Ptm (20). See text for description of points/abbreviations

Abb. 4 **a** Messungen von Po-Pt (7) zwischen Porion und Fossa pterygopalatina sowie Po-Ptm (8) zwischen Porion und Fossa pterygopalatina. **b** Messungen zwischen Porion, Fossa mandibularis und Tuberculum articulare (*AE*): Po-F roof (9), Po-AE mp (10), Po-AE top (11), Po-F post (12). **c** Messungen zwischen Fossa pterygopalatina (Punkt Pt) und Referenzpunkten an Fossa mandibularis und Tuberculum articulare (*AE*): F roof-Pt (13), F post-Pt (14), AE mp-Pt (15), AE top-Pt (16). **d** Messungen zwischen Fossa pterygopalatina (Punkt Ptm) und Referenzpunkten der Fossa mandibularis und dem Tuberculum articulare (*AE*): AE top-Ptm (17), AE mp-Ptm (18), F roof-Ptm (19), F post-Ptm (20). Messpunkte und Abkürzungen s. Text

A total of 20 distances were measured using these reference points.

These 20 measurements were

1. F post-AE top (fossa width),
2. F roof on F post-AE top (fossa depth; [38]; Fig. 3a).

Additionally, the ratio between mandibular fossa depth and width was calculated for each TMJ.

Measurements of the mandibular fossa and the articular tubercle (eminence) were

3. F post-F roof,
4. F post-AE mp,
5. F roof-AE top,
6. AE mp–AE top (Fig. 3b),
7. Po-Pt between porion and pterygopalatine fossa,
8. Po-Ptm between porion and pterygopalatine fossa (Fig. 4a).

From porion to mandibular fossa and to articular tubercle included the distances

9. Po-F roof,
10. Po-AE mp,
11. Po-AE top,
12. Po-F post (Fig. 4b).

From the pterygopalatine fossa (point Pt) to reference points of the mandibular fossa and to articular tubercle included the distances

13. F roof-Pt,
14. F post-Pt,
15. AE mp-Pt,
16. AE top-Pt (Fig. 4c).

From the pterygopalatine fossa (point Ptm) to reference points of the mandibular fossa and to articular tubercle included the distances

17. AE top-Ptm,
18. AE mp-Ptm,
19. F roof-Ptm,
20. F post-Ptm (Fig. 4d).

All visual morphology classifications and measurements on the DTs were performed under constant environmental conditions, including an officially certified image viewing system for radiographic diagnostics.

Statistical analysis

The same blinded examiner remeasured the DTs and repeated the visual classifications of mandibular fossae and condyles after an interval of 3 months. The method error (ME) was then calculated using the Dahlberg formula ($ME = \sqrt{(\sum d^2/2n)}$) [13] where d is the difference of the repeated measurement pairs and n the number of measurements. The ME was <1 for all measurements. Intrarater reliability (IRR) for the visual classification was assessed using Cohen's kappa. For both mandibular fossae and condyles kappa was = 1. Data was recorded using a spreadsheet software (Excel®, Microsoft Corp., Redmond, WA, USA). The Kolmogorov–Smirnov test confirmed normal distribution of the data. Homogeneity of variance was tested using Levene's method. Treatment related changes were analysed with paired Student's t-tests. Descriptive statistics mean (M) and standard deviation (SD) were recorded for each variable. All statistical analyses were performed using SPSS® version 22.0 (IBM Corp., Armonk, NY, USA) for Windows® (Microsoft Corp.). Statistical significance was set at $p < 0.05$.

Results

Visual classification of fossa shape

Visual classification of the sagittal DT slices showed no differences in mandibular fossa shape between T1 and T2 in all 50 mandibular fossae. In 24 patients, fossa shape of the right and left fossa was identical. Only one patient showed side differences of mandibular fossa morphology (patient no. 25; Table 1). In total, 26 of the mandibular fossae were round, 11 ovoid, 5 trapezoid and 8 triangular.

Visual classification of mandibular fossa morphology on tomograms and MRI

Similar visual classification of 50 mandibular fossae were also performed on parasagittal slices of MRI (figure 3 in Kinzinger et al. [25]). No morphological changes were observed. Slightly different to our present investigation, fossa morphology of the right and left TMJ was always the same in each of the 25 patients. The MRI diagnosis also revealed primarily round and ovoid fossa shapes: 34 out of 50 compared to 37 out of 50, respectively, in the present study.

Metrical analysis

Tables 2 and 3 show the results of all measurements. Only few differences between T1 and T2 (ΔT2–T1) were statistically significant ($p < 0.05$). Small treatment related changes ranging from –0.89 mm (decrease) to 1.25 mm (increase) occurred. None of the comparisons between the right and left TMJ were significant (Table 4).

Comparison of linear measurements on tomograms and MRI

Ten of the linear measurements were taken for the same patients on DTs (Figs. 3 and 4b of the present study) and on MRIs (figures 4 and 5 in Kinzinger et al. [25]). DTs and MRIs were taken at comparable points in time, i.e. before and after FMA treatment. The results of our present study (Tables 2 and 3) and the MRI study (tables 3–6 in Kinzinger et al. [25]) were almost identical for 8 of the 10 linear measurements. Only 2 out of 10 linear measurements exhibited minor insignificant differences.

Discussion

We have examined DTs to reveal changes of mandibular fossae after FMA treatment. The patients investigated in our present study were equal to those evaluated in a previous MRI investigation [25]. Hence, direct comparison between results obtained from DTs and MRI scans were possible. This has not been previously published. Therefore, our study adds new data to the literature.

Like other investigators [18, 22], we used DTs to quantify possible transformations of the mandibular fossa after FFA treatment. The patients were positioned within the x-ray unit according to the manufacturer's instructions, using a standard bite block [14]. In agreement with similar studies [37], upper and lower incisors were moved to an edge-to-edge position. The subsequent anterior displacement of the mandible caused anterior and downward movement of the condyles, which ensured complete visual as-

Table 1 Visual classification of mandibular fossa shape
Tab. 1 Visuelle Klassifikation der Kontur der Fossa mandibularis

Patient No.	TMJ Right (R) Left (L)	Fossa shape T1	Diff. R vs L	T2	Diff. R vs L	Change (T1 to T2)
1	R	A	No	A	No	No
	L	A		A		No
2	R	A	No	A	No	No
	L	A		A		No
3	R	A	No	A	No	No
	L	A		A		No
4	R	B	No	B	No	No
	L	B		B		No
5	R	D	No	D	No	No
	L	D		D		No
6	R	B	No	B	No	No
	L	B		B		No
7	R	D	No	D	No	No
	L	D		D		No
8	R	D	No	D	No	No
	L	D		D		No
9	R	B	No	B	No	No
	L	B		B		No
10	R	A	No	A	No	No
	L	A		A		No
11	R	A	No	A	No	No
	L	A		A		No
12	R	A	No	A	No	No
	L	A		A		No
13	R	A	No	A	No	No
	L	A		A		No
14	R	A	No	A	No	No
	L	A		A		No
15	R	A	No	A	No	No
	L	A		A		No
16	R	A	No	A	No	No
	L	A		A		No
17	R	A	No	A	No	No
	L	A		A		No
18	R	D	No	D	No	No
	L	D		D		No
19	R	A	No	A	No	No
	L	A		A		No
20	R	C	No	C	No	No
	L	C		C		No
21	R	A	No	A	No	No
	L	A		A		No
22	R	B	No	B	No	No
	L	B		B		No
23	R	B	No	B	No	No
	L	B		B		No
24	R	C	No	C	No	No
	L	C		C		No

Table 1 (Continued)
Tab. 1 (Fortsetzung)

Patient No.	TMJ Right (R) Left (L)	Fossa shape T1	Diff. R vs L	T2	Diff. R vs L	Change (T1 to T2)
25	R	B	Yes	B	Yes	No
	L	C		C		No
–	50 TMJs	26 round (A)	–	26 round (A)	–	–
		11 oval (B)		11 oval (B)		
		5 trapezoid (C)		5 trapezoid (C)		
		8 triangular (D)		8 triangular (D)		

Fossa shape was classified as A = round, B = oval, C = trapezoidal or D = triangular.
TMJ temporomandibular joint, *T1* timepoint 1, *T2* timepoint 2, *Diff.* difference

Table 2 Measurements within the mandibular fossa and the articular eminence (according to Fig. 3)
Tab. 2 Messungen innerhalb der Fossa mandibularis und des Tuberculum articulare (analog Abb. 3)

Measurement/ratio	T1 M ± SD	T2 M ± SD	Δ T2–T1 M ± SD	*p*-value
F post–AE top (width; 1)				
Right	15.78 ± 3.08	16.64 ± 2.64	0.85 ± 2.66	0.139^{NS}
Left	16.43 ± 2.59	17.25 ± 2.57	0.82 ± 2.29	0.092^{NS}
Total	16.11 ± 2.83	16.95 ± 2.59	0.84 ± 2.59	0.024*
F roof onto F post–AE top (height; 2)				
Right	5.02 ± 1.63	5.35 ± 2.10	0.34 ± 2.03	0.435^{NS}
Left	5.21 ± 1.50	5.23 ± 1.86	0.02 ± 2.08	0.968^{NS}
Total	5.12 ± 1.55	5.29 ± 1.96	0.17 ± 2.04	0.562^{NS}
Ratio height/width				
Right	0.33 ± 0.12	0.32 ± 0.11	–0.01 ± 0.14	0.740^{NS}
Left	0.32 ± 0.09	0.31 ± 0.13	–0.01 ± 0.13	0.647^{NS}
Total	0.32 ± 0.11	0.31 ± 0.12	–0.01 ± 0.13	0.573^{NS}
Ratio width/height				
Right	3.48 ± 1.29	3.73 ± 2.09	0.25 ± 2.33	0.609^{NS}
Left	3.50 ± 1.68	1.47 ± 4.16	1.04 ± 3.61	0.171^{NS}
Total	3.49 ± 1.48	4.14 ± 3.30	0.65 ± 3.04	0.147^{NS}
F post–F roof (3)				
Right	8.36 ± 2.45	8.18 ± 2.30	–0.18 ± 1.68	0.609^{NS}
Left	8.35 ± 1.74	8.64 ± 2.04	0.29 ± 2.36	0.556^{NS}
Total	8.35 ± 2.10	8.41 ± 2.16	0.06 ± 2.04	0.846^{NS}
F post–AE mp (4)				
Right	12.03 ± 2.73	12.28 ± 2.44	0.25 ± 2.11	0.569^{NS}
Left	12.12 ± 1.71	12.88 ± 1.89	0.76 ± 2.08	0.088^{NS}
Total	12.08 ± 2.24	12.59 ± 2.17	0.51 ± 2.09	0.100^{NS}
F roof–AE top (5)				
Right	10.80 ± 2.03	12.04 ± 2.55	1.25 ± 2.79	0.043*
Left	11.49 ± 2.52	12.38 ± 2.72	0.89 ± 2.31	0.065^{NS}
Total	11.16 ± 2.30	12.22 ± 2.62	1.06 ± 2.53	0.005**
AE mp–AE top (6)				
Right	5.26 ± 1.08	5.84 ± 1.49	0.58 ± 1.39	0.046*
Left	5.72 ± 1.19	6.08 ± 1.49	0.35 ± 1.27	0.178^{ns}
Total	5.49 ± 1.15	5.96 ± 1.48	0.47 ± 1.32	0.016*

Treatment-related changes seen for mandibular fossae. Linear measurements in millimeter (mm); ratios without units
M mean, *SD* standard deviation, *NS* not significant, Δ *T2–T1* positive or negative values indicate increases or decreases
$^{*}p < 0.05$; $^{**}p < 0.01$; $^{***}p < 0.001$

Table 3 Measurements of the anatomical structures porion and mandibular fossa (according to Fig. 4)

Tab. 3 Messungen an den anatomischen Strukturen Porion und Fossa mandibularis (analog Abb. 4)

Measurement/ratio	T1 M ± SD	T2 M ± SD	Δ T2–T1 M ± SD	*p*-value
Po–Pt (7)				
Right	52.23 ± 3.80	52.24 ± 3.63	0.01 ± 3.78	0.990^{NS}
Left	52.38 ± 5.68	51.88 ± 4.49	–0.50 ± 4.48	0.617^{NS}
Total	52.31 ± 4.80	52.06 ± 4.04	–0.25 ± 4.11	0.700^{NS}
Po–Ptm (8)				
Right	50.48 ± 3.31	49.60 ± 4.07	–0.89 ± 4.10	0.334^{NS}
Left	51.09 ± 4.93	50.66 ± 4.25	–0.43 ± 4.16	0.644^{NS}
Total	50.78 ± 4.16	50.13 ± 4.11	–0.66 ± 4.09	0.305^{NS}
F roof–Po (9)				
Right	15.38 ± 3.34	14.77 ± 3.02	–0.61 ± 1.76	0.129^{NS}
Left	14.74 ± 2.65	14.41 ± 2.66	–0.33 ± 2.50	0.551^{NS}
Total	15.06 ± 3.00	14.59 ± 2.82	–0.47 ± 2.14	0.163^{NS}
AE mp–Po (10)				
Right	20.79 ± 2.56	20.92 ± 2.62	0.13 ± 1.64	0.713^{NS}
Left	20.59 ± 2.31	20.75 ± 2.23	0.16 ± 1.70	0.666^{NS}
Total	20.69 ± 2.41	20.84 ± 2.41	0.15 ± 1.65	0.564^{NS}
AE top–Po (11)				
Right	25.86 ± 2.27	26.51 ± 2.39	0.66 ± 1.59	0.074^{NS}
Left	26.15 ± 2.25	26.62 ± 1.97	0.48 ± 1.25	0.096^{NS}
Total	26.00 ± 2.23	26.57 ± 2.17	0.57 ± 1.42	0.013*
F post–Po (12)				
Right	12.40 ± 3.46	12.27 ± 3.10	–0.13 ± 1.91	0.764^{NS}
Left	12.20 ± 3.87	12.32 ± 3.79	0.12 ± 2.41	0.822^{NS}
Total	12.30 ± 3.62	12.30 ± 3.41	–0.01 ± 2.14	0.876^{NS}
F roof–Pt (13)				
Right	39.34 ± 2.91	39.98 ± 2.81	0.64 ± 3.29	0.373^{NS}
Left	40.34 ± 4.84	40.31 ± 4.98	–0.03 ± 3.90	0.967^{NS}
Total	39.87 ± 4.04	40.15 ± 4.07	0.28 ± 3.60	0.595^{NS}
F post–Pt (14)				
Right	47.85 ± 3.44	48.60 ± 3.29	0.75 ± 3.26	0.294^{NS}
Left	48.62 ± 5.27	48.60 ± 4.53	–0.02 ± 3.90	0.979^{NS}
Total	48.26 ± 4.46	48.60 ± 3.94	0.35 ± 3.59	0.523^{NS}
AE mp–Pt (15)				
Right	36.40 ± 3.21	35.93 ± 3.49	–0.47 ± 3.38	0.502^{NS}
Left	37.03 ± 4.43	36.72 ± 4.61	–0.31 ± 3.24	0.638^{NS}
Total	36.72 ± 3.85	36.33 ± 4.08	–0.39 ± 3.27	0.411^{NS}
AE top–Pt (16)				
Right	35.46 ± 3.75	35.21 ± 2.98	–0.26 ± 3.63	0.734^{NS}
Left	35.75 ± 4.36	35.30 ± 3.90	–0.45 ± 2.66	0.408^{NS}
Total	35.61 ± 4.03	35.25 ± 3.44	–0.35 ± 3.14	0.434^{NS}
AE top–Ptm (17)				
Right	26.13 ± 2.63	25.35 ± 2.57	–0.78 ± 2.96	0.198^{NS}
Left	26.72 ± 4.17	25.93 ± 3.57	–0.79 ± 3.04	0.207^{NS}
Total	26.43 ± 3.46	25.64 ± 3.09	–0.78 ± 2.97	0.067^{NS}
AE mp–Ptm (18)				
Right	30.09 ± 2.44	29.74 ± 2.41	–0.35 ± 2.64	0.518^{NS}
Left	31.06 ± 4.02	30.42 ± 4.26	–0.64 ± 3.66	0.388^{NS}
Total	30.58 ± 3.33	30.08 ± 3.44	–0.49 ± 3.16	0.273^{NS}

Table 3 (Continued)
Tab. 3 (Fortsetzung)

Measurement/ratio	T1 M ± SD	T2 M ± SD	Δ T2–T1 M ± SD	*p*-value
F roof–Ptm (19)				
Right	35.61 ± 2.63	35.59 ± 2.96	–0.02 ± 3.03	0.974^{NS}
Left	36.30 ± 4.26	36.09 ± 4.83	–0.21 ± 4.16	0.803^{NS}
Total	–0.02 ± 3.03	–0.21 ± 4.16	–0.12 ± 3.62	0.821^{NS}
F post–Ptm (20)				
Right	41.78 ± 2.64	41.94 ± 2.64	0.16 ± 3.42	0.828^{NS}
Left	42.59 ± 4.58	42.74 ± 3.75	0.15 ± 4.45	0.868^{NS}
Total	42.19 ± 3.74	42.35 ± 3.24	0.15 ± 3.94	0.789^{NS}

Treatment-related changes seen for mandibular fossae. Linear measurements in millimeter (mm); ratios without units
M mean, *SD* standard deviation, *NS* not significant, Δ *T2–T1* positive or negative values indicate increases or decreases
$*p < 0.05$; $**p < 0.01$; $***p < 0.001$

Table 4 *P*-value comparison between right and left side
Tab. 4 Vergleich zwischen rechter und linker Seite, *p*-Werte

Measurement/ratio	T1	T2	Δ T2-T1
F post–AE top (width; 1)	0.276^{NS}	0.188^{NS}	0.828^{NS}
F roof onto F post–AE top (height; 2)	0.442^{NS}	0.957^{NS}	0.717^{NS}
Ratio height/width	0.990^{NS}	0.981^{NS}	0.989^{NS}
Ratio width/height	0.916^{NS}	0.990^{NS}	0.459^{NS}
F pos t–F roof (3)	0.968^{NS}	0.366^{NS}	0.421^{NS}
F post–AE mp (4)	0.858^{NS}	0.073^{NS}	0.302^{NS}
F roof–AE top (5)	0.059^{NS}	0.501^{NS}	0.595^{NS}
AE mp–AE top (6)	0.156^{NS}	0.360^{NS}	0.430^{NS}
Po–Pt (7)	0.713^{NS}	0.553^{NS}	0.972^{NS}
Po–Ptm (8)	0.738^{NS}	0.420^{NS}	0.690^{NS}
F roof–Po (9)	0.260^{NS}	0.933^{NS}	0.303^{NS}
AE mp–Po (10)	0.716^{NS}	0.786^{NS}	0.601^{NS}
AE top–Po (11)	0.480^{NS}	0.668^{NS}	0.824^{NS}
F post–Po (12)	0.712^{NS}	0.913^{NS}	0.716^{NS}
F roof–Pt (13)	0.707^{NS}	0.881^{NS}	0.829^{NS}
F post–Pt (14)	0.917^{NS}	0.917^{NS}	0.867^{NS}
AE mp–Pt (15)	0.822^{NS}	0.642^{NS}	0.810^{NS}
AE top–Pt (16)	0.992^{NS}	0.927^{NS}	0.954^{NS}
AE top–Ptm (17)	0.513^{NS}	0.473^{NS}	0.998^{NS}
AE mp–Ptm (18)	0.251^{NS}	0.435^{NS}	0.781^{NS}
F roof–Ptm (19)	0.524^{NS}	0.535^{NS}	0.974^{NS}
F post–Ptm (20)	0.518^{NS}	0.327^{NS}	0.806^{NS}

Overview of *p*-values for different measurements taken on the panoramic tomograms for T1, T2 and Δ T2–T1 for mandibular fossae. Linear measurements in millimeter (mm); ratios without units
NS not significant

sessment of the mandibular fossae without superimposition of anatomical structures, e.g. the zygomatic arc.

We used DTs which were part of diagnostic procedures during fixed orthodontic appliance treatment. This complied with the ALARA (as low as reasonably achievable) principle [15] because no additional radiographic examinations of the patients were conducted. Still, DTs are associated with radiation burden for the patient. On the other hand, MRI is available as a radiation-free alternative. However, recording an MRI is time consuming, costly and not available in the orthodontist's office. Moreover, the comparatively small field of view in an MRI shows only a limited area around the TMJ. Compared to MRI scans, tomograms have the advantage that additional osseous structures anterior and posterior to the mandibular fossa and the articular eminence can be used as reference points for different linear measurements [22]. In our study, we used the porion and the pterygopalatine fossa for this purpose. The distance between these two structures remained stable during the observed treatment period, allowing these to be used

as stable anatomical landmarks. Given that apposition and resorption in the fossae occur in a structured manner, the depth and width of the fossae would reveal no differences in sagittal measurement comparison. This alone does not allow the conclusion that no changes occurred. However, adding measurements of porion and pterygopalatine fossa allows a comparison with stable anatomical landmarks. If the relative position between mandibular fossa and these structures change, a fossa shift could be proven. However, this was not the case in the present tomogram investigation.

Translation of the mandibular fossa has been identified as contributor to mandibular positional changes after FFA treatment in animal studies [31, 32, 39, 51, 52]. Signs of possible fossa remodelling after functional treatment were found in isolated incidents [49]. Other studies described remodelling in the posterior–superior portion of the condyle and/or the fossa on the PT in selected Herbst appliance patients [6, 37].

Bone remodelling is not visible in conventional radiography (PT) until mineralization has occurred. The opposite is true in MRI [43, 45]: cartilage that is formed during treatment is visible. The results of a recent MRI study in the same population [25] did not show any alterations of fossa width or depth. If any remodelling had occurred, it must have happened symmetrically. However, in both the tomogram and the MRI study, distance measurements relating to the porion revealed no changes.

Results of both the tomogram and the MRI investigation do not allow the conclusion that FFA treatment does not alter the mandibular fossa and adjacent regions but indicate that changes are so minuscule that they cannot be recorded with the methods described, or that they occur within methological error.

Ruf and Pancherz [43, 45] have already described that the amount of fossa remodelling accounts for less effect than condyle remodelling. Using dedicated 3D rendering software [29], possible remodelling/alterations of the mandibular fossae might be revealed [25]. To reveal possible age-related influences, further research is needed.

Conclusions

A total of 25 patients with skeletal class II malocclusion were successfully treated with a fixed functional appliance (FMA). The mandibular fossae received pre- and post-treatment metric analysis and visual classification of tomograms, and allow the following conclusions:

- No visible changes in fossa morphology were found in the sagittal plane.
- The majority (24 out of 25) showed bilateral similarity of TMJ structures.
- No metric changes could be recorded for width, depth and ratio thereof, neither between T1 and T2 nor between the different sides.
- No metric changes could be found for another 18 linear parameters, neither between T1 and T2 nor between the different sides.
- There is no indication of a fossa shift.
- Absolute values are identical for tomogram and MRI measurements within the same patient group.

The standard tomographic radiograph appears to be a valuable research tool for the sagittal analysis of mandibular fossa changes during treatment with a fixed functional appliance. Provided that the tomogram is recorded with an x-ray unit adjusted according to the manufacturer's instructions, an additional MRI is not necessary to evaluate sagittal fossa changes.

Compliance with ethical guidelines

Conflict of interest G.S.M. Kinzinger, J.A. Lisson, D. Booth and J. Hourfar declare that they have no competing interests.

Ethical standards Ethical approval for this retrospective study was obtained from the Institutional Review Board (IRB). For this type of study formal consent is not required.

References

1. Aidar LA, Dominguez GC, Yamashita HK, Abrahao M (2010) Changes in temporomandibular joint disc position and form following Herbst and fixed orthodontic treatment. Angle Orthod 80:843–852
2. Alomar X, Medrano J, Cabratosa J, Clavero JA, Lorente M, Serra I, Monill JM, Salvador A (2007) Anatomy of the temporomandibular joint. Semin Ultrasound CT MR 28:170–183
3. Arat ZM, Gokalp H, Erdem D, Erden I (2001) Changes in the TMJ disc-condyle-fossa relationship following functional treatment of skeletal Class II Division 1 malocclusion: a magnetic resonance imaging study. Am J Orthod Dentofacial Orthop 119:316–319
4. Arici S, Akan H, Yakubov K, Arici N (2008) Effects of fixed functional appliance treatment on the temporomandibular joint. Am J Orthod Dentofacial Orthop 133:809–814
5. Bag AK, Gaddikeri S, Singhal A, Hardin S, Tran BD, Medina JA, Curé JK (2014) Imaging of the temporomandibular joint: an update. World J Radiol 6:567–582
6. Bakke M, Paulsen HU (1989) Herbst treatment in late adolescence: clinical, electromyographic, kinesiographic, and radiographic analysis of one case. Eur J Orthod 11:397–407
7. Baltromejus S, Ruf S, Pancherz H (2002) Effective temporomandibular joint growth and chin position changes: Activator versus Herbst treatment. A cephalometric roentgenographic study. Eur J Orthod 24:627–637
8. Bishara SE (2006) Class II malocclusions: diagnostic and clinical considerations with and without treatment. Semin Orthod 12:11–24
9. Caruso S, Storti E, Nota A, Ehsani S, Gatto R (2017) Temporomandibular joint anatomy assessed by CBCT images. Biomed Res Int 2017:2916953

10. Chavan SJ, Bhad WA, Doshi UH (2014) Comparison of temporomandibular joint changes in Twin Block and Bionator appliance therapy: a magnetic resonance imaging study. Prog Orthod 15:57
11. Chintakanon K, Sampson W, Wilkinson T, Townsend G (2000) A prospective study of Twin-block appliance therapy assessed by magnetic resonance imaging. Am J Orthod Dentofacial Orthop 118:494–504
12. Crow HC, Parks E, Campbell JH, Stucki DS, Daggy J (2005) The utility of panoramic radiography in temporomandibular joint assessment. Dentomaxillofac Radiol 34:91–95
13. Dahlberg G (1940) Statistical methods for medical and biological students. Interscience Publications, New York.
14. Dentsply Sirona Bensheim (2017) Patient positioning with standard bite block for the perfect panoramic image. http://manuals.sirona.com/home.HomeDmsDocument.download.html?id=5947;. Accessed 9 Aug 2017
15. Eastman TR (2013) ALARA and digital imaging systems. Radiol Technol 84:297–298
16. Franco AA, Yamashita HK, Lederman HM, Cevidanes LH, Proffit WR, Vigorito JW (2002) Frankel appliance therapy and the temporomandibular disc: a prospective magnetic resonance imaging study. Am J Orthod Dentofacial Orthop 121:447–457
17. Guner DD, Ozturk Y, Sayman HB (2003) Evaluation of the effects of functional orthopaedic treatment on temporomandibular joints with single-photon emission computerized tomography. Eur J Orthod 25:9–12
18. Hansen K, Pancherz H, Petersson A (1990) Long-term effects of the Herbst appliance on the craniomandibular system with special reference to the TMJ. Eur J Orthod 12:244–253
19. Ivorra-Carbonell L, Montiel-Company J-M, Almerich-Silla J-M, Paredes-Gallardo V, Bellot-Arcís C (2016) Impact of functional mandibular advancement appliances on the temporomandibular joint—a systematic review. Med Oral Patol Oral Cir Bucal 21:e565–e572
20. Katsavrias EG (2003) The effect of mandibular protrusive (activator) appliances on articular eminence morphology. Angle Orthod 73:647–653
21. Katsavrias EG (2006) Morphology of the temporomandibular joint in subjects with Class II Division 2 malocclusions. Am J Orthod Dentofacial Orthop 129:470–478
22. Katsavrias EG, Voudouris JC (2004) The treatment effect of mandibular protrusive appliances on the glenoid fossa for Class II correction. Angle Orthod 74:79–85
23. Kinzinger G, Kober C, Diedrich P (2007) Topography and morphology of the mandibular condyle during fixed functional orthopedic treatment—a magnetic resonance imaging study. J Orofac Orthop 68:124–147
24. Kinzinger G, Gülden N, Roth A, Diedrich P (2006) Disc-condyle Relationships during Class II Treatment with the Functional Mandibular Advancer (FMA). J Orofac Orthop 67:356–375
25. Kinzinger G, Hourfar J, Kober C, Lisson J (2018) Mandibular fossa morphology during therapy with a fixed functional orthodontic appliance—a magnetic resonance imaging study. J Orofac Orthop 79:116–132
26. Kinzinger G, Ostheimer J, Förster F, Kwandt PB, Reul H, Diedrich P (2002) Development of a new fixed functional appliance for treatment of skeletal class II malocclusion first report. J Orofac Orthop 63:384–399
27. Kinzinger GS, Roth A, Gülden N, Bücker A, Diedrich PR (2006) Effects of orthodontic treatment with fixed functional orthopaedic appliances on the condyle-fossa relationship in the temporomandibular joint: a magnetic resonance imaging study (Part I). Dentomaxillofac Radiol 35:339–346
28. Kinzinger GS, Roth A, Gülden N, Bücker A, Diedrich PR (2006) Effects of orthodontic treatment with fixed functional orthopaedic appliances on the disc-condyle relationship in the temporomandibular joint: a magnetic resonance imaging study (Part II). Dentomaxillofac Radiol 35:347–356
29. Kober C, Hayakawa Y, Kinzinger G, Gallo L, Otonari-Yamamoto M, Sano T, Sader RA (2007) 3D-visualization of the temporomandibular joint with focus on the articular disc based on clinical T1-, T2-, and proton density weighted MR images. Int J CARS 2:203–210
30. LeCornu M, Cevidanes LHS, Zhu H, Wu C-D, Larson B, Nguyen T (2013) Three-dimensional treatment outcomes in class II patients treated with the Herbst appliance: a pilot study. Am J Orthod Dentofacial Orthop 144:818–830
31. McNamara JA Jr., Carlson DS (1979) Quantitative analysis of temporomandibular joint adaptations to protrusive function. Am J Orthod 76:593–611
32. McNamara JA Jr. (1973) Neuromuscular and skeletal adaptations to altered function in the orofacial region. Am J Orthod 64:578–606
33. Pancherz H, Ruf S, Kohlhas P (1998) "Effective condylar growth" and chin position changes in Herbst treatment: a cephalometric roentgenographic long-term study. Am J Orthod Dentofacial Orthop 114:437–446
34. Pancherz H, Michailidou C (2004) Temporomandibular joint growth changes in hyperdivergent and hypodivergent Herbst subjects. A long-term roentgenographic cephalometric study. Am J Orthod Dentofacial Orthop 126:153–161
35. Pancherz H, Fischer S (2003) Amount and direction of temporomandibular joint growth changes in Herbst treatment: a cephalometric long-term investigation. Angle Orthod 73:493–501
36. Pancherz H (1979) Treatment of class II malocclusions by jumping the bite with the Herbst appliance. A cephalometric investigation. Am J Orthod 76:423–442
37. Paulsen HU (1997) Morphological changes of the TMJ condyles of 100 patients treated with the Herbst appliance in the period of puberty to adulthood: a long-term radiographic study. Eur J Orthod 19:657–668
38. Pullinger AG, Seligman DA (2001) Multifactorial analysis of differences in temporomandibular joint hard tissue anatomic relationships between disk displacement with and without reduction in women. J Prosthet Dent 86:407–419
39. Rabie AB, Zhao Z, Shen G, Hagg EU, Dr O, Robinson W (2001) Osteogenesis in the glenoid fossa in response to mandibular advancement. Am J Orthod Dentofacial Orthop 119:390–400
40. Richter U, Richter F (2004) An MRI-monitored investigation of the condyle-fossa relationship during Herbst appliance treatment. Orthodontics (Chic) 1:43–51
41. Ruf S, Baltromejus S, Pancherz H (2001) Effective condylar growth and chin position changes in activator treatment: a cephalometric roentgenographic study. Angle Orthod 71:4–11
42. Ruf S, Pancherz H (1998) Kiefergelenkswachstumsadaptation bei jungen Erwachsenen während Behandlung mit der Herbst-Apparatur. Eine prospektive magnet-resonanztomographische und kephalometrische Studie. Inf Orthod Kieferorthop 30:735–750
43. Ruf S, Pancherz H (1998) Temporomandibular joint growth adaptation in Herbst treatment: a prospective magnetic resonance imaging and cephalometric roentgenographic study. Eur J Orthod 20:375–388
44. Ruf S, Pancherz H (1998) Long-term TMJ effects of Herbst treatment: a clinical and MRI study. Am J Orthod Dentofacial Orthop 114:475–483
45. Ruf S, Pancherz H (1999) Temporomandibular joint remodeling in adolescents and young adults during Herbst treatment: A prospective longitudinal magnetic resonance imaging and cephalometric radiographic investigation. Am J Orthod Dentofacial Orthop 115:607–618
46. Ruf S, Pancherz H (2000) Does bite-jumping damage the TMJ? A prospective longitudinal clinical and MRI study of Herbst patients. Angle Orthod 70:183–199

47. Ruf S (2003) Short- and long-term effects of the Herbst appliance on temporomandibular joint function. Semin Orthod 9:74–86
48. Ruf S, Bendeus M, Pancherz H, Hagg U (2007) Dentoskeletal effects and "effective" temporomandibular joint, maxilla and chin changes in good and bad responders to van Beek activator treatment. Angle Orthod 77:64–72
49. Ruf S (2001) Einfluß der Herbst-Apparatur auf Kiefergelenkwachstum und -funktion. Eine klinische, magnetresonanztomographische und kephalometrische Studie. Zahnmed. Habil. Gießen.
50. Serbesis-Tsarudis C, Pancherz H (2008) "Effective" TMJ and chin position changes in Class II treatment. Angle Orthod 78:813–818
51. Voudouris JC, Woodside DG, Altuna G, Kuftinec MM, Angelopoulos G, Bourque PJ (2003) Condyle-fossa modifications and muscle interactions during herbst treatment, part 1. New technological methods. Am J Orthod Dentofacial Orthop 123:604–613
52. Voudouris JC, Woodside DG, Altuna G, Angelopoulos G, Bourque PJ, Lacouture CY, Kuftinec MM (2003) Condyle-fossa modifications and muscle interactions during Herbst treatment, Part 2. Results and conclusions. Am J Orthod Dentofacial Orthop 124:13–29
53. Wadhawan N, Kumar S, Kharbanda OP, Duggal R, Sharma R (2008) Temporomandibular joint adaptations following two-phase therapy: an MRI study. Orthod Craniofac Res 11:235–250
54. Watted N, Witt E, Kenn W (2001) The temporomandibular joint and the disc-condyle relationship after functional orthopaedic treatment: a magnetic resonance imaging study. Eur J Orthod 23:683–693
55. Yildirim E, Karacay S, Erkan M (2014) Condylar response to functional therapy with Twin-Block as shown by cone-beam computed tomography. Angle Orthod 84:1018–1025